Desalination and Water Treatment
www.deswater.com

doi: 10.5004/dwt.2022.28079

247 (2022) 294–308
January

Eggshell derived calcium oxide nanoparticles for Toluidine blue removal

Edwin A. Ofudje[a,*], Ezekiel F. Sodiya[a], Fatai Akinwunmi[b], Abimbola A. Ogundiran[c], Olugbenga B. Oladeji[d], Oluremi A. Osideko[d]

[a]*Department of Chemical Sciences, Mountain Top University, Prayer City, Ogun State, Nigeria, emails: ofudjeandrew4real@yahoo.com/eaofudje@mtu.edu.ng/ofudje@gmail.com (E.A. Ofudje), efsodiya@mtu.edu.ng (E.F. Sodiya)*
[b]*Department of Chemical Sciences, Federal University of Agriculture, Abeokuta, Ogun State, Nigeria, email: akinwunmifatai2@gmail.com*
[c]*Department of Chemical Sciences, Tai Solarin University of Education, Ijebu-Ode, Ogun State, email: ogundiranaa@tasued.edu.ng*
[d]*Department of Chemistry, Federal University of Agriculture, Abeokuta, Ogun State, Nigeria, emails: oladejiolugbenga@yahoo.com (O.B. Oladeji), osidekooluremi@yahoo.com (O.A. Osideko)*

Received 10 September 2021; Accepted 18 December 2021

ABSTRACT

Agro-waste of eggshells was successfully used to prepared calcium oxide nanoparticles via thermal decomposition at a calcination temperature of 700°C and was found to be an ideal adsorbent for Toluidine blue (TB) dye adsorption. The structural examination of the as-prepared adsorbent was achieved with several analytical procedures such as scanning electron microscopy, transmission electron microscopy, Fourier-transform infrared spectroscopy, X-ray diffraction, thermogravimetric analysis/differential thermal analysis, and zeta potential. The influence of pH, contact time, concentration of contaminant, sorbent dose, as well as temperature on the elimination of TB was studied in a series of batch processes. The kinetic investigation of the experiments revealed that the uptake of Toluidine blue by the adsorbent obeyed pseudo-second-order kinetics model with rate constants given as 2.761×10^4, 7.770×10^4, 8.350×10^4, 7.590×10^4 and 6.140×10^4 (g mg^{-1} min^{-1}), while the equilibrium data agreed with both the two- and three-parameter isotherms tested. The utmost adsorption capacity (Q_{max}) of the Langmuir isotherm obtained was 114.151 mg g^{-1}, while its counterpart from the Freundlich isotherm (K_F) found was 17. 173 (mg/g)(mg/L)$^{-1/2}$. Thermodynamic parameters evaluation revealed that the elimination of TB is endothermic, spontaneous and feasible in nature.

Keywords: Adsorption; Toluidine; Eggshell; Equilibrium; Kinetics; Thermodynamics

1. Introduction

Water is of critical importance not only to the natural ecosystem but also to human developments [1]. However, water contamination as a result of growing environmental contamination from manufacturing industries particularly from developing nations like Nigeria is a major disquiet. Industries like textile, paper, dye factories, food additives, and plastic industries utilized dyes to add colour to their products, and the effluent is often released into the water system without proper treatment [1–2]. It is reported that the existence of a tiny quantity of dyes (<1 ppm) in water is very

* Corresponding author.

much visible, unwanted which impedes the transmission of light in water bodies containing coloured effluent [1]. Impediment of light penetration into water body may equally affect the photosynthetic activity in aquatic life [3–4]. Reactive dyes consist of azo-based chromophore in conjunction with different kinds of reactive groups and they have the ability to attach to textile fibers forming covalent bonds which makes their eradication of immense significance [5–6]. Despite their numerous usages and applications, dyes have created much anxiety owning to their toxic property. Toluidine blue (TB) is a basic thiazine metachromatic dye also known as Tolonium chloride or TBO which is primarily used in the manufacture of dyestuffs, although it is also used in histology, forensic examination, renal pathology, neuropathology, in the production of rubber, chemicals, pesticides and as a curing agent for epoxy resin systems [7–9]. In spite of the numerous biological importance of TB, it could also be harmful. Its harmful effects could arouse from either direct contact or ingestion and its effects could vary depending on the duration and quantity of exposure [7–9]. The principal signs of toxicity following acute and short-term exposure to this chemical are that haemoglobin which carries oxygen in the blood changes to methaemoglobinaemia resulting in a decreased supply of oxygen to peripheral tissues and related effects in the spleen [7–8]. There are also cases of bladder cancer recorded in a thorough, well conducted retrospective cohort study at a rubber chemical plant in upstate New York [9]. Other notable health challenges associated with Toluidine are irritation in the skin and eyes, nausea, vomiting, abdominal pain, diarrhea, and burning on urination [7–9].

Over the past few decades, quite a lot of methods like ion exchange, oxidation, coagulation, flocculation, membrane separation, and many more have been documented in the treatment of wastewater [1–6]. However, these methods had suffered some setbacks such as the generation of sludge, the elevated cost of operation, and restoration of adsorbate and adsorbent seems impossible. More also, dyes structure normally consists of complex aromatic structures, thus making them highly stable and very hard to biodegrade and as such, biological treatment of wastewater seems inept in decontaminating dye contaminated wastewater [1]. Adsorption which is a physical process of treatment is prefers over other methods due to its simplicity (does not require highly skilled manpower or sophisticated equipment), no pre-treatment requirement, applicability to a wide variety of pollutants (both organic and inorganic), and no toxic by-products formation [10]. The cost-effectiveness of adsorption process depends largely on the nature of the adsorbent material used and as such, researchers are always in the search of a cheap and efficient material. In the search for novel adsorbents, quit arrays of materials and their modified products have been researched. Several adsorbents such as Turkish zeolite [11], fly ash [12], gypsum [13], water-insoluble starch sulfate [14], orange peel [15], MnO_2/ZnO [16] and MnO_2/Al_2O_3 [16] had been reported for their vast ability to eliminate Toluidine dye in wastewater. The continuous search for inexpensive and excellent adsorbents for the treatment of wastewater necessitated this study.

Nanocrystalline metal oxides have gained momentous awareness as excellent sorbents for the treatment of chlorinated and phosphorus-containing compounds, toxic gases, and HCl [17]. Calcium oxide (CaO) is a very useful and important industrial compound which is found useful in several applications such as photocatalyst for organic pollutants [18], nanosize semiconductor [19], antibacterial agent [20], detoxification of pollutant [21], catalyst [22], and in the conservation of wall paint [23]. Calcium oxide has excellent reactivity and adsorption properties and as such could be used in the purification of contaminated water. Several synthetic methods such as co-precipitation method [21], sol–gel method [23], and thermal decomposition method [24] have been reported for the preparation of CaO. We reported the synthesis of CaO nanoparticles via one step thermal decomposition of eggshells. In the past, the use of CaO in the water industry has been limited to the correction of solution pH and in some cases as a coagulant to aid the process of coagulation/flocculation [25]. Eggshell is a porous material in nature and contains large amount of $CaCO_3$ embedded within polysaccharides and proteins, while eggshell membrane (ESM) mainly contains fibrous proteins [26]. There are several reports on the usefulness of eggshell waste amongst which are to increase the mineral content of compost, biodiesel, as fertilizer, cement additive to increase its strength, to deter slugs and snails, as a feed for aviary birds [27]. The structure of eggshells is known to consist of about 85% to 95% of $CaCO_3$ and the remaining 5% is made up of magnesium carbonate (0.3%) and calcium phosphate (0.3%) [28]. However, in this study, eggshells which are often discarded as waste materials were utilized as a precursor for the production of calcium oxide nanoparticle adsorbent via thermal decomposition of the shell. The structure of the eggshell derived calcium oxide nanoparticles adsorbent was thereafter investigated with the aid of X-ray diffraction (XRD), Fourier-transform infrared spectroscopy (FT-IR), scanning electron microscopy (SEM), field-emission scanning electron microscopy (FE-SEM), transmission electron microscopy (TEM), and thermogravimetric analysis (TGA). The as-prepared adsorbent was contacted with Toluidine dye in aqueous solution via batch process; while the adsorption data were studied with kinetics and isotherm models.

2. Adsorbent preparation

Waste chicken eggs were sourced from a poultry farm and cleansed using distilled water for impurities elimination. The shells were thereafter boiled in a beaker containing 10% NaOH for 20 min and rinsed using distilled water. The eggshells were oven-dried at 70°C for 12 h and thereafter pulverized in mortar and pestle to form fine powders. The powdered eggshells were subjected to heat treatment in a muffle furnace at 700°C in three-stage heating and soaking to form the eggshell derived calcium oxide nanoparticle (EDCON). Airtight container was used to keep the product obtained before characterization and served as adsorbent. Flow chart for the synthesis of eggshell derived calcium oxide nanoparticle and the TB sorption process is represented in Fig. 1.

2.1. Characterization

The functional groups available on the exterior of the precursor and the prepared adsorbent before and

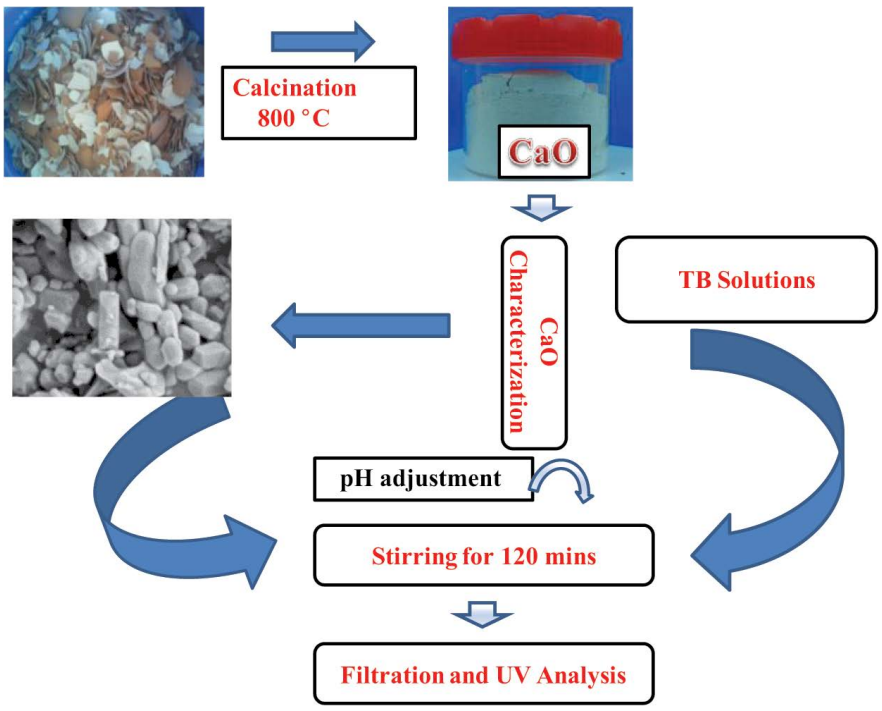

Fig. 1. Flow chart for the synthesis of CaO from eggshell for TB adsorption.

after adsorption were identified with FT-IR spectrometer TENSOR 27 spectrometer (Bruker, Germany) using KBr pellet procedure. Samples of EDCON were mixed with KBr powder and compressed to form a pellet. FT-IR spectrum was achieved between 400–4,000 cm^{-1}. Information relating to the morphology was obtained via FE-SEM using Carl Zeiss AG (Supra 55VP) with an accelerated voltage of 5–30 kV with Au sputtered sample and also confirmed with TEM which was performed with a Tecnai G2 20 FEI (Netherland). The phase purity of the prepared adsorbent was measured with Bruker D8 Advance X-ray Diffractometer, using CuKα (1·5406 Å). The measurement was made in the range of 10°–60° on 2θ with a step size of 0.05°. TGA was done with the aid of SDT Q600 V8.3 Build 101 simultaneous DSC-TGA instrument for the determination of the thermal stability. Surface area, pore size, and pore volume analyses were done using a Quantachrome NOVA 2200C (USA) particle size analyzer. The particle size distribution present in the prepared adsorbent was measured using a NANOTRAC equipped with Microtrac FLEX 10.5.2 software.

2.2. Equilibrium experiments

TB stock solutions were made by sonicating calculated amount of TB in Millipore water to achieve the desired concentration. For TB adsorption, 10 mL of TB was measured into a 100 mL beaker and the pH adjustment was done by introducing a negligible portion of 0.1 M of either NaOH or HCl. Thereafter, 30 mg of EDCON adsorbent was introduced and the content was equilibrated for 120 min. The aliquot was removed using a syringe and the concentration of dye was determined with a UV-Vis spectrophotometer at 630 nm wavelength.

The removal amount and percentage adsorption (R %) was estimated by adopting Eqs. (1) and (2):

$$Q_e = \frac{C_o - C_e}{m} \times V \tag{1}$$

$$\%R = \frac{C_o - C_e}{C_o} \times 100 \tag{2}$$

where Q_e denotes the quantity of TB adsorbed onto the adsorbent surface at equilibrium (mg g^{-1}), the solution volume is represented as V (L), while the mass of EDCON is designated as m (g). Experiments were performed in triplicate, and mean value was recorded.

Two-parameter isotherms like Freundlich, Temkin, Langmuir, and Dubinin–Radushkevich (D-R) as well as three-parameter isotherms like Redlich–Peterson (R-P) and Sips isotherms were deployed to evaluate the equilibrium data as described in Eqs. (3)–(8) [29–36]:

$$Q_{eq} = K_F C_e^{1/n} \tag{3}$$

$$Q_e = \frac{RT}{b_T} \ln a_T C_e \tag{4}$$

$$Q_e = \frac{Q_o b C_e}{1 + b C_e} \tag{5}$$

$$Q_e = Q_m e^{-\beta \varepsilon^2} \tag{6}$$

$$Q_e = \frac{Q_o C_e}{1 + K_R C_e^g} \quad (7)$$

$$Q_e = \frac{Q_s (K_s C_e)^{\beta_s}}{1 + (K_s C_e)^{\beta_s}} \quad (8)$$

The amount of adsorbate in the bulk as well as the amount adsorbed at equilibrium can be successfully described using isotherms. The Langmuir isotherm parameter Q_o (mg g^{-1}) denotes the monolayer adsorption capacity, while b (L mg^{-1}) stands for the adsorption energy. The separation factor (R_L) from the Langmuir isotherm was obtained from the expression: $R_L = 1/1 + bC_o$ with values in the range of 0 to 1 indicating favorable adsorption, whereas, values of $R_L > 1$ inferred unfavorable adsorption and $R_L = 0$ indicates irreversible adsorption [29,32]. The parameters K_F (mol/g)(mol/L)$^{-1/n}$ represents the capacity of adsorption while n (g L^{-1}) denotes the intensity of adsorption from the Freundlich isotherm. The binding constant (L g^{-1}) as well as the heat of adsorption (J mol^{-1}) from the Temkin isotherm are given as quantities α_T and β_T respectively. From the D-R isotherm, the theoretical saturation capacity is represented as Q_m (mol g^{-1}), the Polanyi potential ε (J mol^{-1}) can be expressed as: $\varepsilon = RT\ln(1 + 1/C_e)$, where R and T standard constants. The parameter β provides information about the mean free energy E (kJ mol^{-1}) and it can be represented by the relationship: $E = 1/\sqrt{2\beta}$. If the value of E lies between 8 and 16 kJ mol^{-1}, it signify chemisorption process, but when E is fewer than 8 kJ mol^{-1}, it inferred physisorption process [30,33]. From the three-parameter isotherms, Redlich–Peterson parameters K_R, (L g^{-1}) and g stand for the equilibrium constant and exponent which range between 0 and 1. Langmuir and Freundlich isotherms can both be deduced from the value of β. For instance, if β = 1, the relation becomes Langmuir isotherm but when β = 0, it indicates Freundlich isotherm equation. Sips parameter constants K_s, Q_s, and β_s are the equilibrium constant (L mg^{-1}), sorption capacity (mg g^{-1}), and the exponent which lies between 0 and 1 [34–36].

2.3. Kinetic investigations

The kinetics of the adsorption study was evaluated by contacting 10 mL of TB in a 100 mL beaker with 30 mg of EDCON and agitated using a temperature controlled orbital shaker at a speed of 150 rpm. Thereafter, samples were taken at different time gaps (0, 10, 30, 60, 90, 120, 150, and 180 min) using a syringe, and the dye concentration was evaluated at 630 nm with a spectrophotometer. The amounts of TB adsorbed at time t, Q_t (mg g^{-1}) which represents adsorption capacity per unit mass of the adsorbent was computed using Eq. (9):

$$Q_t = \frac{C_o - C_t}{m} \times V \quad (9)$$

where C_o (mg L^{-1}) and C_t (mg L^{-1}) representing the concentration of TB at time $t = 0$ and $t = t$ respectively, V denotes solution volume of dye (L), and m (g) stands for the mass of EDCON utilized. Pseudo-first-order, pseudo-second-order, Elovich, and intraparticle diffusion kinetic models were engaged in describing the solid/liquid adsorption systems as listed in Eqs. (10)–(13) [37–40]:

$$Q_t = Q_e\left(1 - e^{-k_1 t}\right) \quad (10)$$

$$Q_t = \frac{k_2 Q_e^2 t}{1 + k_2 Q_e t} \quad (11)$$

$$q_t = \frac{1}{\beta}\left(\ln \alpha\beta\right) + \left(\frac{1}{\beta}\right)\ln t \quad (12)$$

$$Q_t = K_{\text{id}} t^{0.5} + C_i \quad (13)$$

where Q_e and Q_t denoting the quantity of TB sorbed in mg g^{-1} at equilibrium and at time t, while the rate constants of pseudo-first-order and pseudo-second-order kinetic models are k_1 (min^{-1}) and k_2 (g mg^{-1} min^{-1}) respectively. From the Elovich model, α and β signify the adsorption and desorption rates in mg g^{-1} min^{-1} respectively, while the rate constant of the intraparticle diffusion model is given as K_{id} (mg g^{-1} min$^{-0.5}$) and C_i is the intercept which is a measure of the surface thickness of the adsorbent. The least-square fit plots against t were utilized to estimate all the constants.

2.4. Statistical test

The sum of error squares (SSE, %) was deployed to further ascertain the best fit among the various kinetics models used in this study [30]:

$$\%\ \text{SSE} = \sqrt{\frac{\left(\left(Q_{(\text{exp})} - Q_{(\text{Cal})}\right)/Q_{\text{exp}}\right)^2}{N-1}} \times 100 \quad (14)$$

where the data point number represented as N. The greater the values of R^2 and the fewer the values of SSE, the more satisfactory the model.

2.5. Desorption study

The desorption of TB dye from the surface of EDCON was investigated by treating the TB-loaded EDCON with 0.2 M aqueous solution of acetic acid. The mixture was separated and analyzed for TB content. The percentage of desorption was performed from the Eq. (15):

$$\%d_e = \frac{\text{Cd}_{\text{de}}}{\text{Cd}_{\text{ad}}} \times 100 \quad (15)$$

with d_e signifying desorption, Cd_{ad} and Cd_{de} are the amount of pollutant adsorbed and desorbed in mg g^{-1}, respectively.

3. Results and discussion

3.1. Characterization

Table 1 represents the physical parameters of the synthesized calcium oxide nanoparticles. Concerning

the values provided in Table 1, the surface area, average pore size, pore volume, and bulk density are found to be 124.56 $m^2\ g^{-1}$, 2.41 nm, 0.29 $cm^3\ g^{-1}$, and 2.35 g cm^{-3}, respectively. Fig. 2 depicts the FT-IR spectrum of the precursor, synthesized EDCON before and after adsorption. The spectrum of the precursor show prominent bands at 715, 856, 1,463 and 3,593 cm^{-1} corresponding to the main peaks of $CaCO_3$. The wave numbers at 715 and 856 cm^{-1} belong to v_4 in plane band and v_2 out of plane band of Ca–O bond [41,42]. The peak observed at 1,463 cm^{-1} (v_3 anti-symmetric stretching) belongs to C–O stretching of calcite, while the band appearing at 1,765 cm^{-1} was assigned to C=O of carbonate ion [41,42]. The broadband at 3,593 cm^{-1} was assigned to the –OH group from moisture since $CaCO_3$ is hydrophilic in nature [41,42]. For the synthesized adsorbent, the peak at 586 cm^{-1} is assign to Ca–O bonds, the characteristic absorption bands for carbonate ions (CO_3^{2-}) were observed at 755, 876 and 1,478 cm^{-1} respectively. The band observed at 1,047 cm^{-1} denotes the C–O band, while the peaks found at 3,604 cm^{-1} are assign to the stretching of OH– which is due to the absorbed water [42]. After the adsorption of TB, however, the initial peaks observed at 586; 876; 1,047; 1,478 and 3,604 cm^{-1} were observed to have reduced to 564; 865; 1,034; 1,455 and 3,597 cm^{-1}, respectively indicating their involvement in the adsorption process of TB. The observed differences in the peak shifting as well disappearance of peaks reflect the nature of the relationship between the surface functional groups of EDCON and the adsorbed TB species which is due to the electrostatic interactions reflecting the changes in bond strength thus resulting in band shifts to lower frequencies.

Table 1
Physical parameters of synthesized EDCON

Parameters	EDCON
Surface area ($m^2\ g^{-1}$)	124.56
Average pore size (nm)	2.41
Pore volume ($cm^3\ g^{-1}$)	0.29
Bulk density (g cm^{-3})	2.25
Ash content (%)	4.56
pH_{ZPC}	5.52

Fig. 3 shows the XRD pattern of the raw eggshell, synthesized EDCON before and after adsorption. The raw eggshell was indexed to calcite powder (JCPDS file no: 47-1743). Some of the planes observed are (104), (012), (110), (113), (202), (018), and (116). For the prepared adsorbent, the XRD pattern shows a single phase of calcium oxide powder as indexed by JCPDS file no. 37-1497 with the appearance of peaks at 2θ = 32°, 37.23° and 54.06° corresponding to (111), (200), and (220) planes respectively. After the adsorption process, a decrease in peak intensity and slight shift in peak positions were observed which is due to the incorporation of the pollutant into the crystal

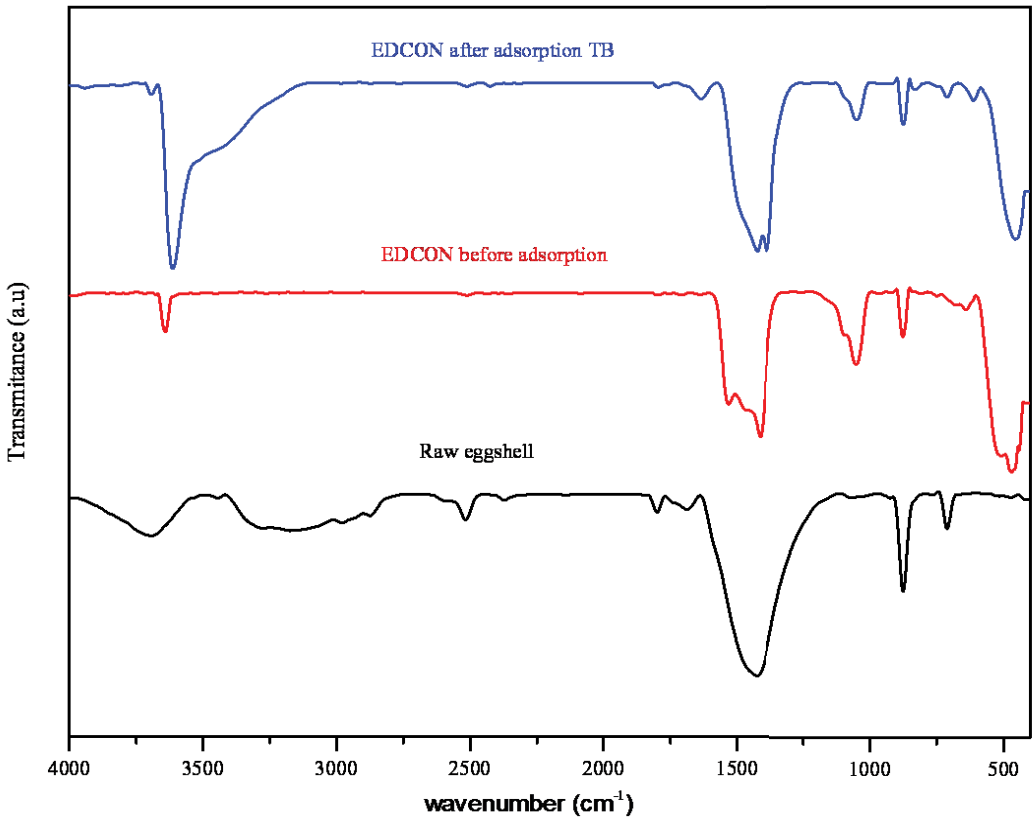

Fig. 2. FT-IR results showing raw eggshell, synthesized EDCON before and after adsorption.

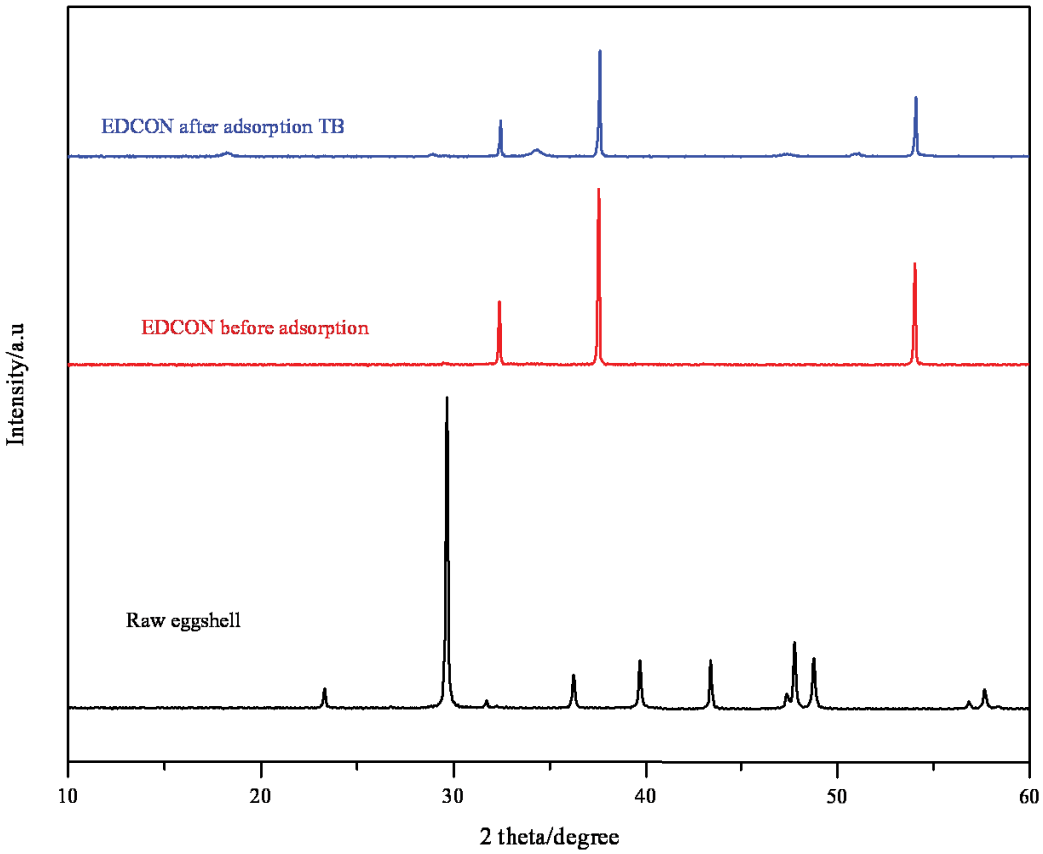

Fig. 3. XRD results showing raw eggshell, synthesized EDCON before and after adsorption.

lattice of the adsorbent (EDCON). TGA curve (Fig. 4a) shows 10% weight loss at 110°C which could be as a result of the disappearance of moisture from the calcite, 15.6% weight loss at 498°C which is due to the loss of organic contents, and a final weight loss of 18.8% at 690°C and was attributed to the decomposition of $CaCO_3$ (which is the structure of the eggshell) to form CaO. After this, there was no further weight loss. The distribution of the particle size of EDCON is represented in Fig. 4b showing the majority of the particles in the range of 0.4–0.75 μm. Fig. 5 depicts the FE-SEM images of (a) raw eggshell, (b) synthesized EDCON before adsorption, (c) synthesized EDCON after adsorption, and (d) TEM and SAED of EDCON synthesized. The morphology of the raw eggshell revealed a flower-like structure, that of the CaO fabricated shows different shapes of rod-like and round crystals of size in the range of 3–53 nm long and 5–12 nm wide (Fig. 5b). FE-SEM investigation of the EDCON (Fig. 5c) after adsorption revealed an agglomerated pattern which could be due to the soaking of the powder in the pollutant. TEM evaluation confirmed the FE-SEM results of the EDCON particles to consist of different shapes of rod-like and round crystals (Fig. 5d).

3.2. *Effects of agitation time and dye concentration*

The role of agitation time on the uptake of TB by the prepared adsorbent was examined for periods from 10 to 220 min as presented in Fig. 6. The rate of dye adsorption rose rapidly with the contact time and reduced gradually as it approaches equilibrium. The maximum contact time required to arrive at equilibrium is 120 min after which no further appreciable adsorption process was noticed. The fast uptake at the early stage is as a result of the availability of the large number of vacant sites on the surface of EDCON which increases with the amount of TB accumulated on the adsorbent within the first 120 min. However, after the adsorption of TB onto the vacant sites, subsequent TB uptake becomes complicated as a result of the revolting forces between the adsorbed TB molecules and the remaining TB in the aqueous solution. Related observations were documented in the literature [25,29]. The influence of contact duration on the adsorption of Toluidine blue by neem leaf powder as reported by Himanshu and Vashi [43] showed continuously increased in Toluidine adsorption with a rise in contact duration from 30 to 480 min. This was attributed to the adsorbent large surface area at the beginning of the reaction process. Sibel et al. [44] reported that the amount of Toluidine sorbed onto clinoptilolite rose with an increase in both the initial concentration of Toluidine and reaction times with equilibrium reached at 30 min. It was observed further that the amount of Toluidine adsorbed was 9.4×10^{-5} mol g^{-1} at a concentration of 3.0×10^{-3} M and pH of 7.0. Also, Rauf et al. [45] studied the adsorption of TB on gypsum and found that equilibrium time was reach at 60 min. Investigating the role of the concentration of pollutants on the sorption

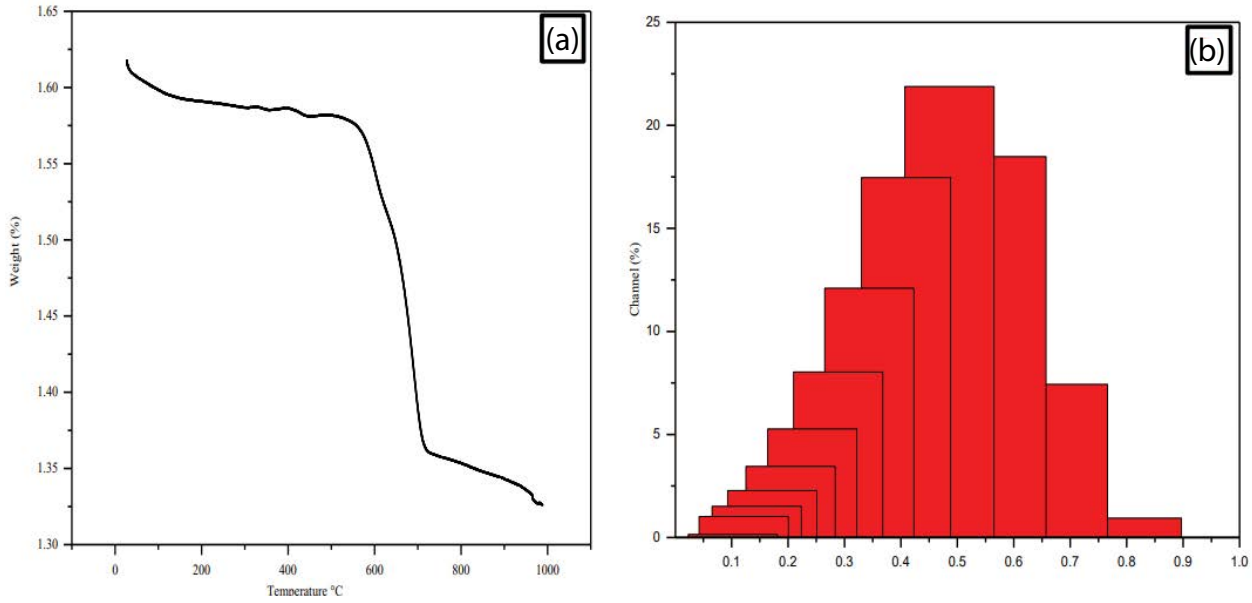

Fig. 4. Plots of (a) TGA of raw eggshell and (b) particle size of synthesized EDCON powder.

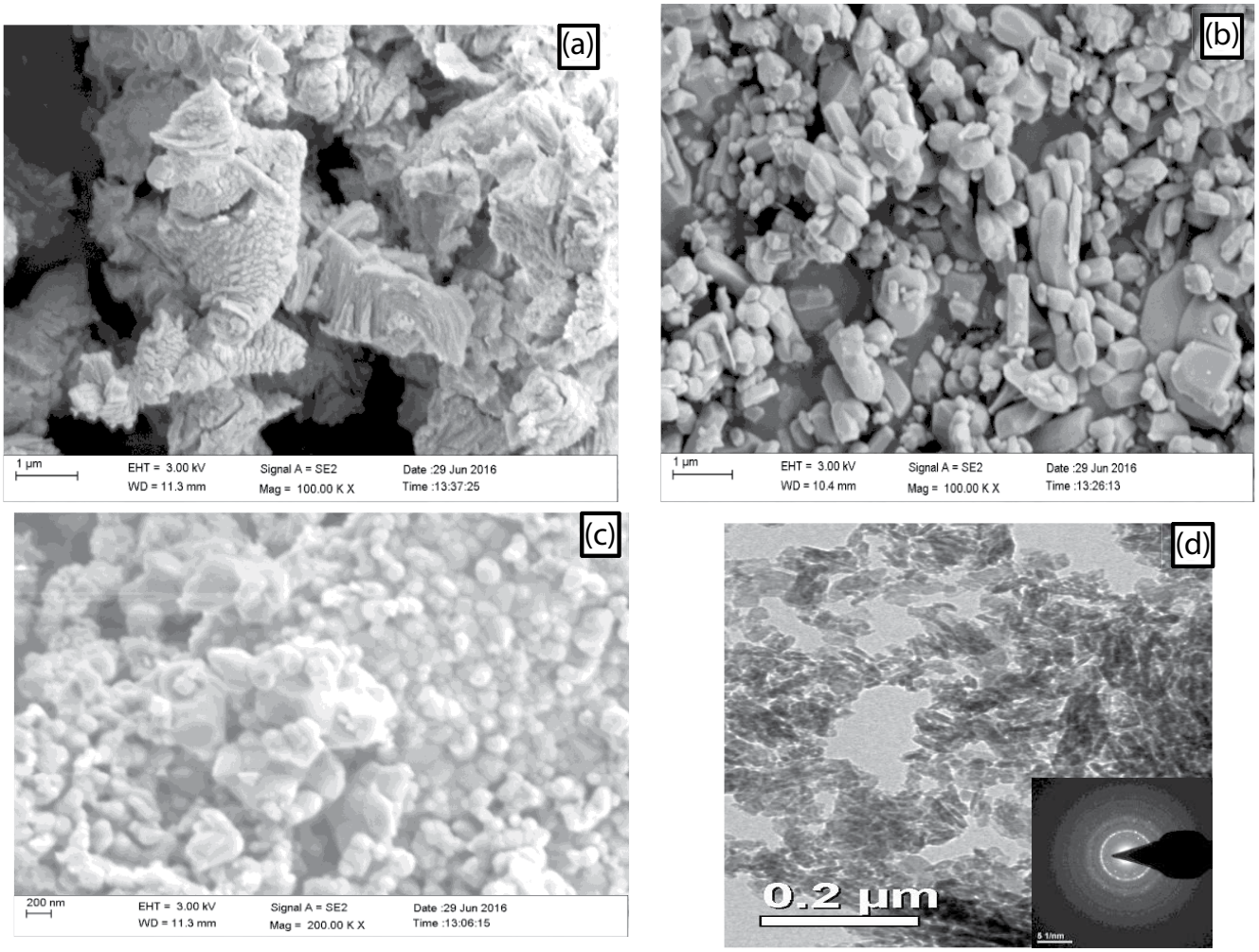

Fig. 5. FE-SEM images of (a) raw eggshell, (b) synthesized EDCON before adsorption, (c) synthesized EDCON after adsorption and (d) TEM and SAED of EDCON.

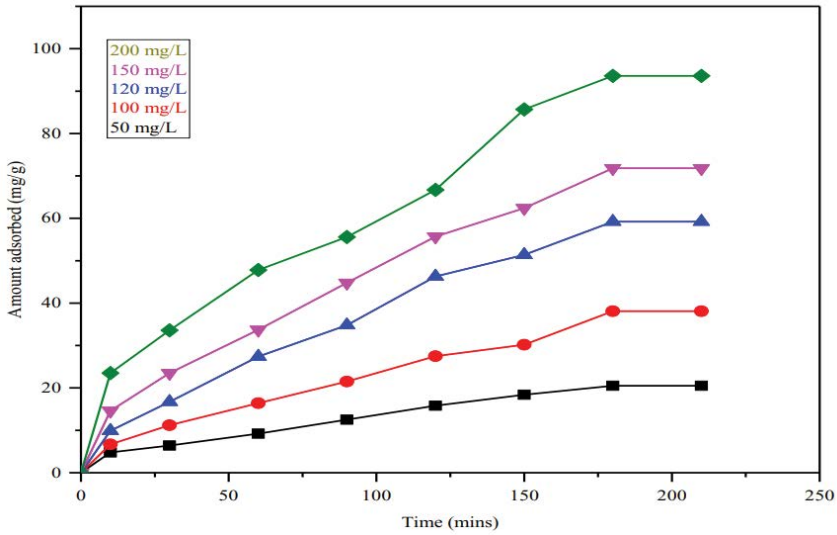

Fig. 6. Plots of the effects of contact time and initial adsorbate concentration on the adsorption of TB by EDCON.

process is a significant factor for overcoming mass transfer resistance of the solute (pollutant) from the aqueous phase to the solid phase. The effect of different initial TB concentrations on the sorption capacity of EDCON adsorbent was investigated as listed in Fig. 6. The removal efficiency of TB increased with the dye concentration. This is because higher concentrations of pollutants lead to an enhanced concentration gradient, which, in turn, results in greater chances of collision among the dye molecules and the active sites of adsorption of EDCON and thus increase the adsorption process [29,31].

3.3. Effects of hydrogen ion concentration and adsorbent dosage

Solution pH in the adsorption process has been recognized as a vital variable governing the uptake of pollutants from contaminated solution onto adsorbents surface. Literature reports had it that hydrogen ions themselves are strong competitors for the negatively charged adsorbent surface coupled with the ionization of functional groups of both the adsorbate and adsorbent [29,32,43–45]. Different batch experiments were performed within the solution pH of 3 to 9 in other to assess the role of pH on the elimination of TB as presented in Fig. 7b. It was observed that the quantity of TB adsorbed onto the EDCON surface increased with the solution pH up to 6.0 with maximum uptake of 95.3%. At low pH, hydrogen ions vie for the available sites on the surface of EDCON along with the dye molecule due to protonation and as such, the surface charge on the adsorbent becomes repulsive and thus hinders the trapping of the cationic dye. However, as the pH increases, deprotonation occurs leading to the surface acquiring more negative charges which result in electrostatic attractions between TB molecules and the adsorbent and thus enhanced the adsorption process. The adsorption capacity was observed to have decreased at a solution pH above 6.

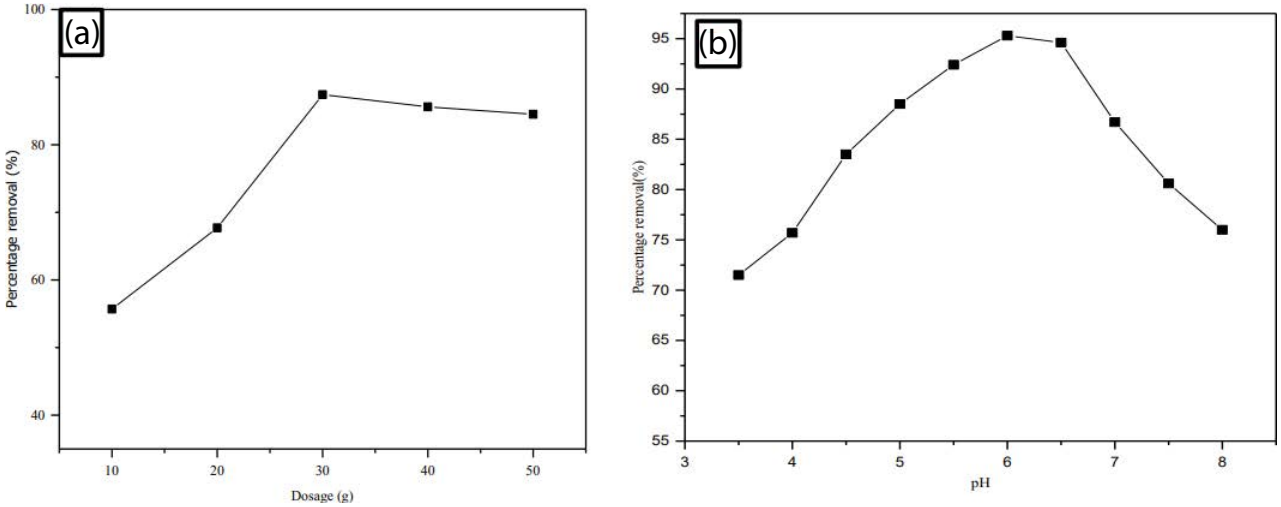

Fig. 7. Effect of (a) EDCON dosage and (b) solution pH on the adsorption of TB.

The pH_{ZPC} of the EDCON as indicated in Table 1 was found to be 5.52 and with the pH values higher than that of pH_{ZPC}, the EDCON surface becomes negatively charged and this enhances the uptake of the dye. Himanshu and Vashi [43] reported a stable or minor increase in the pH range of 1 to 5 when Toluidine dye was adsorbed onto neem leaf powder, however, the colour decolorization increases in aqueous solution as pH increases from 7 to 11. Sibel et al. [44] used Turkish zeolite to recover TB from aqueous solution and reported an increased in the amount of TB sorbed with rise in the solution pH and reached a maximum level of 2.1×10^{-4} mol g^{-1} at a solution pH of 11.0. According to a report by Lei et al. [46], the adjustment of pH value above 6.0 results in the amidocyanogen groups of TB becoming less positive, which reduces the adsorption capacity. Similar reports were presented in the literature by Ahmad [47] in the uptake of crystal violet dye; Barka et al. [48] in the adsorption of SBL dye and by Khalid et al. [49] for the adsorption of yellow 27 respectively. The maximum adsorption percentage of TB onto gypsum was attained at the pH value of 6.5 as discussed by Rauf et al. [45]. They noted that further increase in the pH values resulted in the reduction of the adsorption value and this they attributed to the fact that at superior pH values, surplus hydroxide ions vie for the adsorption sites on the adsorbent surface with dye ions which resulted in reduced adsorption.

The adsorption capacity of EDCON for TB was examined by varying the amount of adsorbent from 10 to 50 mg. Fig. 7a shows the quantity of TB eliminated from aqueous solution and it presents a two-step process with a fast initial adsorption stage at a dosage of 10–20 mg and then followed by much slower gradual adsorption at 30 mg of adsorbent dosage as it approaches equilibrium. The adsorption equilibrium was attained at EDCON dose of 30 mg after which there was no observable increase in the uptake of TB molecules from the aqueous solution. This initial rise in the adsorption capacity is as a result of the available active surface on the adsorbent [29,47].

3.4. Kinetic study

To examine the kinetic mechanism of Toluidine uptake onto EDCON surface from the aqueous phase, pseudo-first-order, pseudo-second-order, Elovich, and intraparticle diffusion kinetic models were employed. The parameters of tested kinetic models were computed using the various equations and Table 2 summarized their values. Models suitability was justified by contrasting the correlation coefficient, (R^2) values of all the models tested and based on this, the correlation coefficient for the tested models confirmed that the pseudo-second-order kinetic model best describes the kinetic data for the elimination of TB onto EDCON surface with the value of (R^2 = 0.993, 0.998, 0.990 and 0.998) for pseudo-first-order, pseudo-second-order, intraparticle diffusion, and Elovich kinetic models respectively. On this basis, it can be assumed that the process of adsorption is predominantly chemisorption which involves the distribution of electrons between TB molecules and the adsorbent surface [50,51]. More also, the calculated adsorption capacity ($Q_{e,cal}$) from the pseudo-second-order model agrees well with the experimental adsorption capacity ($Q_{e,exp}$) when cross-checked with those from pseudo-first-order (Table 2). Also, the linear fitting results of the TB adsorption process onto EDCON derived adsorbent conforms to the Elovich model, which implies that the TB adsorption process could be explained by chemisorption. Furthermore, the intraparticle diffusion model was tested to identify the mechanism of diffusion of TB uptake from aqueous solution onto the active pore size of the adsorbent. Literature reports have it that adsorption mechanism involve three steps with the first step involving the diffusion of solute (pollutants) residue from the liquid phase (adsorbate) to the adsorbent external surface, the second step is the diffusion of the solute into the active pores of the adsorbent surface and finally, the adsorption of the solute residue on the adsorbent internal surface [51–54]. It is believed that pollutant initial concentration as well as

Table 2
Kinetic parameters of the adsorption of TB by EDCON

	C_o (mg L^{-1})	50	100	120	150	200
	$Q_{e,exp}$ (mg g^{-1})	23.130	47.122	71.221	90.800	112.061
	$Q_{e,cal}$ (mg g^{-1})	24.099	52.393	76.853	96.794	119.496
First-order	k_1 (min^{-1})	0.152	0.133	0.151	0.157	0.157
	R^2	0.969	0.990	0.993	0.948	0.978
	% SSE	0.014	0.037	0.026	0.022	0.020
	$Q_{e,cal}$	21.596	45.829	68.857	87.300	107.660
Second-order	$k_2 \times 10^4$ (g mg^{-1} min^{-1})	2.761	7.770	8.350	7.590	6.140
	R^2	0.991	0.997	0.998	0.994	0.993
	% SSE	0.022	0.009	0.011	0.013	0.015
	K_{id} (mg g^{-1} $min^{-1/2}$)	4.748	6.223	14.756	20.899	25.764
Intraparticle diffusion	C (mg g^{-1})	1.392	3.095	4.416	5.513	6.825
	R^2	0.968	0.981	0.964	0.966	0.990
	α (mg g^{-1} min^{-1})	0.470	0.715	1.170	1.594	2.031
Elovich	β (g mg^{-1})	0.654	0.293	0.125	0.085	0.066
	R^2	0.996	0.997	0.996	0.998	0.997

contact time could affect the first stage, while the last stage is regarded as a rate-determining step. It was observed that the diffusion of the solute onto the external surface was relatively very fast in the first min, while the intraparticle diffusion phase was speedily accomplished and persistent up to 120 min. Lastly, the adsorption phase occurs when the TB molecules are slowly adsorbed on the active surface sites and are retained in the pores. It can be deduced that the process of adsorption mechanism involves a multifaceted process and that the rate-controlling step was not determined by only the intraparticle diffusion kinetics model. The values obtained from the intercept of the plots gave an insight into the boundary layer thickness since greater intercept inferred a higher boundary layer effect [49,51–54].

3.5. Adsorption isotherms

Evaluation of isotherm data with either empirical or theoretical equations is important in describing the working parameters governing the adsorption methods. From the two-parameters isotherms: D-R, Freundlich, Temkin, and Langmuir models were deployed to evaluate their physical values as shown in Table 3. The correlation coefficient R^2 (0.994, 0.990, 0.994, and 0.996) of D-R, Freundlich, Temkin and Langmuir suggests excellent harmony between the theoretical values and experimental results for all the models tested, while the extent of the exponent 1/n of the Freundlich and the separation factor R_L of the Langmuir isotherm suggest favorable adsorption process of the adsorbent. Freundlich isotherm is usually used to explain adsorption processes that span over a range of concentrations and assume surface heterogeneity distribution of active sites and energies [51]. Maximum adsorption capacity, Q_m, and the adsorption affinity b calculated from Langmuir equation are 114.151 mg g^{-1} and 0.066 L mg^{-1}, respectively. From the Freundlich model, the utmost adsorption capacity (K_F) obtained is 17.173 (mg/g) $(mg/L)^{-1/2}$, while the adsorption constants for D-R isotherm are 45.317 mg g^{-1} for Q_m, 10.221 mol^2 J^{-2} for ε and 11.810 kJ mol^{-1} for E respectively. The E value falls within the range of ion-exchange mechanism since the value lies within 8–16 kJ mol^{-1} which implies the involvement of some chemical relationships between the TB and EDCON surface [31,50]. The results for three-parameter isotherms as analyzed are provided in Table 3, while the modeled isotherms are given in Fig. 8b. The values of K_s obtained is 0.235 (L mg^{-1}), while the value of Q_s obtained is 54.824 (mg g^{-1}) for R-P and Sips isotherms respectively (Table 3). Judging from the values of R^2 obtained the three-parameters isotherms tested fit perfectly with the adsorption data of TB uptake by EDCON. Table 4 presents the comparison of adsorption capacities of EDCON with other adsorbents for Toluidine adsorption as reported in the literature and it can be seen that EDCON demonstrates the excellent ability for the removal of Toluidine.

Table 3
Physical isotherm parameters for TB adsorption by EDCON powders

Isotherms	Parameters	EDCON
Langmuir	Q_{max} (mg g^{-1})	114.151
	R_L	0.060
	b (L mg^{-1})	0.066
	R^2	0.996
Freundlich	K_F (mg/g) $(mg/L)^{-1/2}$	17.173
	n	1.622
	R^2	0.990
Temkin	α_T (L g^{-1})	0.587
	β_T (J mol^{-1})	52.564
	R^2	0.994
Dubinin–Radushkevich	Q_m (mg g^{-1})	45.317
	ε $(J\ mol)^2$	10.221
	E (kJ mol^{-1})	11.870
	R^2	0.968
Redlich–Peterson	Q_o (mg g^{-1})	56.821
	K_R, $(mg^{-1}\ L)^{1/g}$	0.335
	g	0.157
	R^2	0.994
Sips	Q_s (mg g^{-1})	54.824
	K_s, (L mg^{-1})	0.235
	β_s	1.014
	R^2	0.996

3.6. Thermodynamic evaluation

The enthalpy change (ΔH), free energy change (ΔG), and entropy change (ΔS) were computed in order to examine the thermodynamic feasibility of the adsorption of TB onto EDCON. The equilibrium constant, K_d can be described in terms of concentrations distribution of solute in solution and adsorbed solute according to the following equation:

$$K_d = \frac{\text{solute}_{\text{adsorbed}}}{\text{solute}_{\text{solution}}} \tag{16}$$

Table 4
Comparison of adsorption capacities of EDCON with other adsorbents for Toluidine adsorption

Adsorbents	Q_{max} (mg g^{-1})	References
Turkish zeolite	33.03	11
Fly ash	6	12
Gypsum	26	13
Water-insoluble starch sulfate	40	14
Orange peel	313.4	15
MnO_2/ZnO	0.54	16
MnO_2/Al_2/O_3	0.11	16
EDCON	114.151	This study

The relationship among these properties were evaluated from:

$$\Delta G^\circ = -RT\ln K_d \tag{17}$$

$$\ln K_d = \frac{\Delta S^\circ}{R} - \frac{\Delta H^\circ}{RT} \tag{18}$$

The plots of InK_d against 1/T (K) produced a linear graph with slope given as $\Delta H^\circ/R$ and intercept as $\Delta S^\circ/R$, while the values got are as shown in Table 5. The ΔH and ΔS calculated are 17.05 and 51.13 kJ mol^{-1} respectively. Free energy values obtained were negative and this indicates spontaneous nature of the uptake process of TB by EDCON with the negative value raising with temperature, while the positive value of ΔH means that the uptake of TB is endothermic and this was further corroborated with the values of the equilibrium constant (K_d) which increases with the temperature. The small positive ΔS value observed suggests a small raise in the extent of randomness at the solid–liquid boundary during the adsorption process. The effect of the temperature on TB adsorption as reported

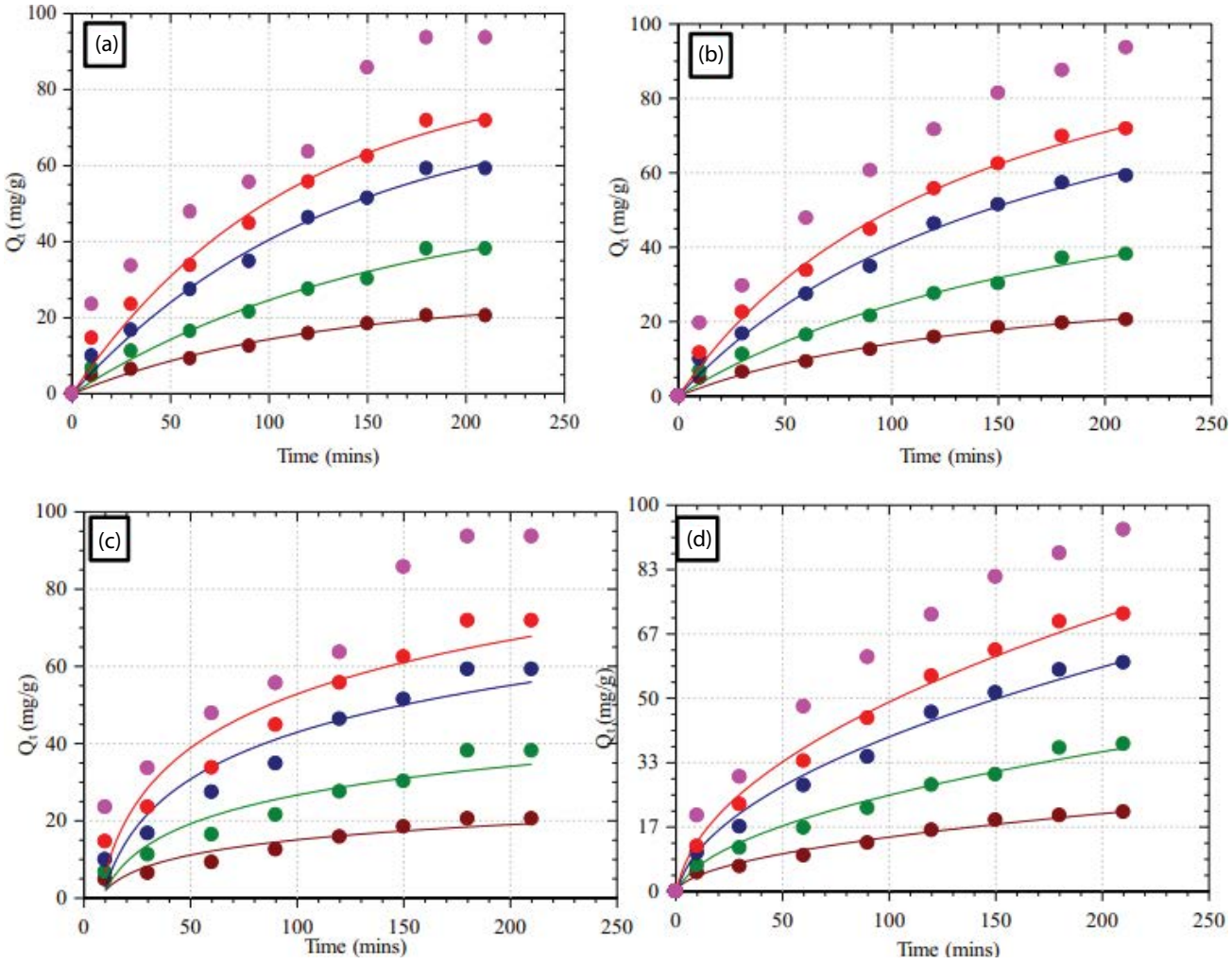

Fig. 8. Plots of (a) pseudo-first-order, (b) pseudo-second-order, (c) Elovich and (d) intraparticle diffusion kinetic models for the adsorption of TB by EDCON.

Table 5
Thermodynamic parameters for TB adsorption by EDCON powders

T (K)	K_d	ΔG (kJ mol^{-1})	E_a (kJ mol^{-1})	ΔH (kJ mol^{-1})	ΔS (kJ mol^{-1})	R^2
303	1.01	–26.82	28.63	17.05	51.13	0.97
308	1.09	–45.11				
313	1.16	–64.02				
318	1.32	–71.21				

by Sibel et al. [44], showed that the removal of TB by clinoptilolite increased from 9.4 × 10^{-5} to 1.68 × 10^{-4} mol g^{-1} when the temperature was increased from 30°C to 40°C.

3.7. Desorption study

The viability of the synthesized calcium oxide adsorbent for likely renewal was evaluated using 0.5 M acetic acid as a desorbing agent and the result is as given in Fig. 9. The desorption percentages for the dye decreased from 83.4% to 62.1% as the reuse number of the adsorbent increases. This implies that the adsorbent obtained from waste eggshell can be successfully reused up to four times or even more.

3.8. Cost analysis of the adsorbent

The waste chicken shell material used as the precursor for the synthesis of the nano-adsorbent has no much significant commercial value in international market. The waste chicken shells were sourced from a poultry farm at

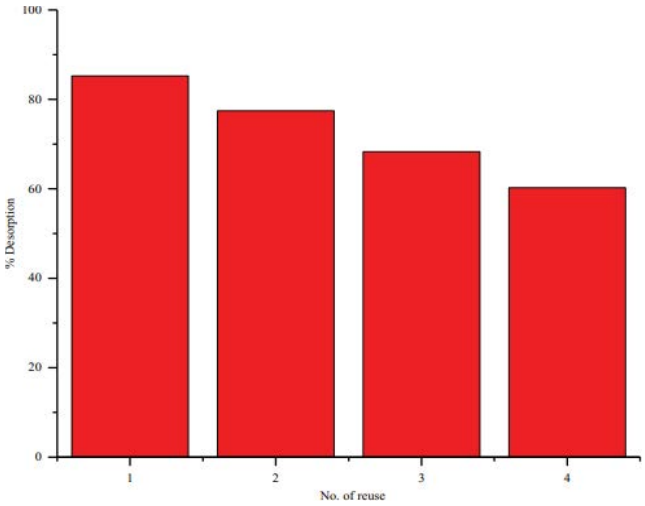

Fig. 9. Plot of desorption percentage against number of reuse of the adsorbent.

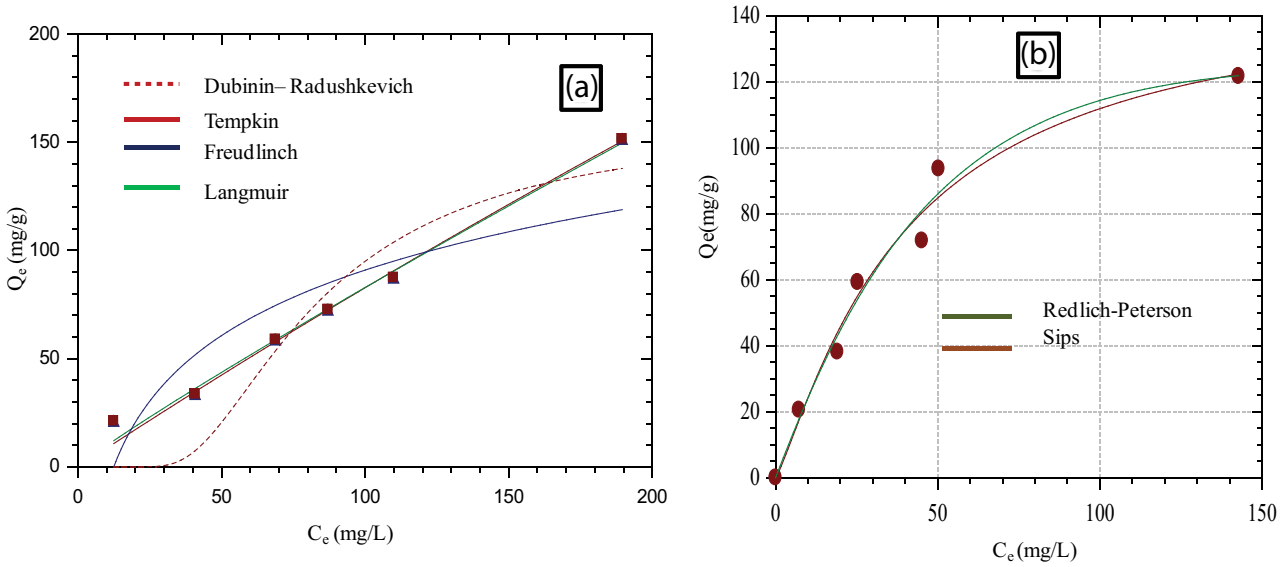

Fig. 10. Plots of (a) two-parameters isotherms and (b) three-parameters isotherms for the adsorption of TB by eggshell derived CaO nanoparticle.

Table 6
Cost analysis of the adsorbent

Adsorbents	Saturation capacity	Price/g of adsorbent compared to EDCON	Price/adsorbed g of TB compared to EDCON	References
Degreased coffee beans	55.3	0.027	0.041	[55]
Fe-BDC MOF	36.419	1	1	[56]
H_2dtoaCu	165.83	18.87	4.14	[57]
IFMC-2	2.4	28.28	429.19	[58]
CAC Merck	222.22	1	1	[59]
Carbonaceous material	75.1	0.14	0.57	[60]
Eggshell derived calcium oxide nanoparticle (EDCON)	114.151	12.33	56.21	This study

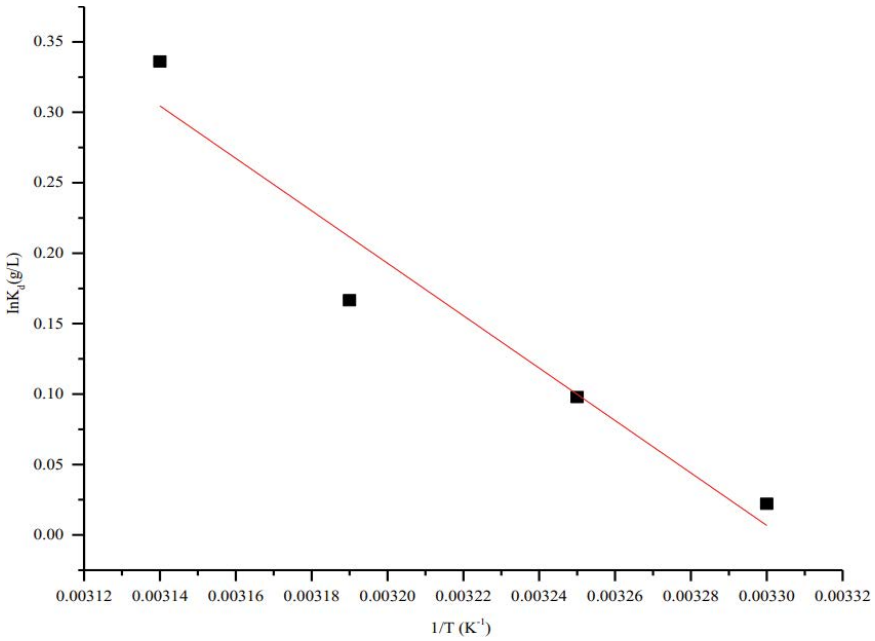

Fig. 11. Thermodynamic plots for the adsorption of TB by eggshell derived CaO nanoparticle.

no cost except for the stipend given for the collection and transportation. However, we strongly believe that the total cost of nano-adsorbent prepared from waste shells will be very low when compared with activated carbon as well as several other adsorbents. By adopting the method reported by Baek et al. [55], a brief appraisal of the cost analysis of using EDCON in the adsorption of TB was done in relation to adsorption saturation capacity of EDCON without taking cognizance of other cost factors such as regeneration or the cost of disposal exhausted adsorbent. Other adsorbents saturation capacity values from the isotherm data where compared with EDCON and the cost analysis of the EDCON revealed that the adsorption process is relatively cost effective for adsorbing 1 kg of TB dye as shown in Table 6 which some authors have adopted in estimating the cost analysis of adsorption system [55–60].

4. Conclusions

Calcium oxide (CaO) derived from thermal decomposition of animal waste of eggshell was employed as cheap and eco-friendly adsorber in the elimination of Toluidine blue (TB) dye via batch adsorption process under different variables like initial dye concentration, biomass dosage, temperature, contact time, and pH of the solution. The adsorption experiments revealed that the quantity of TB dye adsorbed increased with the contact time. Data from equilibrium investigation demonstrate conformity with all the tested isotherms but Langmuir and Sips isotherms showed the best fit when two- and three-parameter isotherms were deployed. Also, data from the kinetic investigation were governed by the model prescribed by pseudo-second-order kinetic. The various characterization techniques like XRD, SEM, TEM, and FT-IR used to investigate the physicochemical and morphological property of the EDCON produced confirmed the formation of different shapes of nanocrystalline EDCON. Report from the thermodynamic investigation of TB uptake revealed negative values of ΔG which infers that the uptake of TB was thermodynamically reasonable and spontaneous; while positive values of ΔH revealed the endothermic character of the adsorption process. Thus, eggshells were successfully utilized as a precursor for the production of calcium oxide adsorbent via thermal decomposition of the shell and deployed in the adsorption of Toluidine blue from aqueous solution.

Acknowledgments

Authors are thankfully for the monetary supports from the Government of India through the Department of Science and Technology for the award of RTF-DC to Ofudje E.A. We equally wish to convey our appreciations to the technical staff of CSIR-CECRI, Central Instrumentation Facility staff such as Ms. Nalini and Mr. R. Ravishankar who are in-charge of SEM as well as Mr. A. Rathish Kumar in-charge of TEM, Karaikudi, Tamil Nadu, India for their help and support.

Conflicts interest

Authors declared that no conflicts of interest.

References

[1] T.V. Ramachandra, N. Ahalya, R.D. Kanamadi, Biosorption: Techniques and Mechanisms, Technical Report: 110, Energy and Wetlands Research Group, Centre for Ecological Sciences, Indian Institute of Science, Bangalore 560 012. Available at: http://wgbis.ces.iisc.ernet.in/biodiversity/pubs/ces_tr/TR110/index.htm

[2] I.M. Banat, P. Nigam, D. Singh, R. Marchant, Microbial decolorization of textile-dye-containing effluents: a review, Bioresour. Technol., 58 (1996) 217–227.

[3] E.A. Clarke, R. Anliker, Organic Dyes and Pigments, R. Anliker, G.C. Butler, E.A. Clarke, U. Förstner, W. Funke, C. Hyslop, G. Kaiser, C. Rappe, J. Russow, G. Tölg, M. Zander, V. Zitko, Eds., Anthropogenic Compounds, The Handbook of Environmental Chemistry Book Series (HEC, Volume 3/3A), Springer Nature, Switzerland, 1980, pp. 181–215.
[4] Y. Fu, T. Viraraghavan, Fungal decolorization of dye wastewater, Bioresour. Technol., 79 (2000) 251–262.
[5] S. Sumathi, B.S. Manju, Uptake of reactive dyes by *Aspergillus foetidus*, Enzyme Microb. Technol., 27 (2000) 347–355.
[6] Z. Aksu, S. Tezer, Equilibrium and kinetic modeling of biosorption of Remazol Black B. by *Rhizopus arrhizus* in a batch system: effect of temperature, Proc. Biochem., 36 (2000) 431–439.
[7] U.S. Department of Health and Human Services, Hazardous Substances Data Bank (HSDB, Online Database), National Toxicology Information Program, Bethesda, National Library of Medicine, MD, 1997.
[8] G.D. Clayton, F.E. Clayton, Eds., Patty's Industrial Hygiene and Toxicology, Volume IIA, 3rd Revised ed., John Wiley & Sons, New York, 1981.
[9] E. Ward, A. Carpenter, S. Markowitz, D. Roberts, W. Halperin, Excess number of bladder cancers in workers exposed to ortho-toluidine and aniline, J. Natl. Cancer Inst., 83 (1991) 501–506.
[10] J. Mittal, Recent progress in the synthesis of layered double hydroxides and their application for the adsorptive removal of dyes: a review, J. Environ. Manage., 295 (2021) 113017, doi: 10.1016/j.jenvman.2021.113017.
[11] S.K. Alpat, O. Ozbayrak, S. Alpat, H. Akçay, The adsorption kinetics and removal of cationic dye, Toluidine blue O, from aqueous solution with Turkish zeolite, J. Hazard. Mater., 151 (2008) 213–220.
[12] R.Y. Talman, G. Atun, Effects of cationic and anionic surfactants on the adsorption of Toluidine blue onto fly ash, Colloids Surf., A, 281 (2006) 15–22.
[13] M.A. Rauf, S.M. Qadri, S. Ashraf, K.M. Al-Mansoori, Adsorption studies of Toluidine blue from aqueous solutions onto gypsum, Chem. Eng. J., 150 (2009) 90–95.
[14] G. Lei, G. Li, J. Liu, S. Ma, J. Zhang, Kinetic and equilibrium studies on adsorptive removal of Toluidine blue by water-insoluble starch sulfate, J. Chem. Eng. Data, 56 (2011) 1875–1881.
[15] L. Ridha, R. Souad, H. Amor, Removal of Toluidine blue from aqueous solution using orange peel waste (OPW), Desal. Water Treat., 56 (2015) 2754–2765.
[16] K.A. Ahmed, Study the effects influencing the adsorption of Toluidine blue O (TBO) dye onto MnO_2 surface, Nat. J. Chem., 30 (2008) 306–322.
[17] I.V. Mishakov, A.F. Bedilo, R.M. Richards, V.V. Chesnokov, A.M. Volodin, V.I. Zaikovskii, R.A. Buyanov, K.J. Klabunde, Nanocrystalline MgO as a dehydrohalogenation, J. Catal., 206 (2002) 40–48.
[18] I.H.N.B. Singh, Green synthesis of nanoparticles and its potential application, Biotechnol. Lett., 38 (2016) 545–560.
[19] C. Bhavya, K. Yogendra, A study on the synthesis, characterization and photocatalytic activity of CaO nanoparticle against some selected azo dyes, Indian J. Appl. Res., 5 (2015) 361–365.
[20] E.A. Münchow, D. Pankajakshan, M.T.P. Albuquerque, K. Kamocki, E. Piva, R.L. Gregory, M.C. Bottino, Synthesis and characterization of CaO-loaded electrospun matrices for bone tissue engineering, Clin. Oral Invest., 20 (2016) 1921–1933.
[21] M. Sadeghi, M.H. Husseini, A novel method for the synthesis of CaO nanoparticle for the decomposition of sulfurous pollutant, J. Appl. Chem. Res., 7 (2013) 39–49.
[22] M.R. Joya, J.H.B. Ruiz, A.M. Raba, Quicklime as an alternative in the photodegradation of contaminants, J. Phys. Conf. Ser., 687 (2016) 12044, doi: 10.1088/1742-6596/687/1/012044.
[23] O. Darčanova, A. Beganskiene, A. Kareiva, Sol-gel synthesis of calcium nanomaterial for paper conservation, Chemija, 26 (2015) 25–31.
[24] N. Tangboriboon, R. Kunanuruksapong, A. Sirivat, Preparation and properties of calcium oxide from eggshells via calcination, Mater. Sci.-Pol., 30 (2012) 313–322.
[25] N.A. Oladoja, I.A. Ololade, S.E. Olaseni, V.O. Olatujoye, O.S. Jegede, A.O. Agunloye, Synthesis of nano calcium oxide from a gastropod shell and the performance evaluation for Cr(VI) removal from aqua system, Ind. Eng. Chem. Res., 51 (2012) 639–648.
[26] A. Mittal, M. Teotia, R.K. Soni, J. Mittal, Applications of eggshell and eggshell membrane as adsorbents: a review, J. Mol. Liq., 223 (2016) 376–387.
[27] B. Haddad, A. Mittal, J. Mittal, A. Paolone, D. Villemin, M. Debdab, G. Mimanne, A. Habibi, Z. Hamidi, M. Boumedienea, B. El-Habib, Synthesis and characterization of eggshell (ES) and eggshell with membrane (ESM) modified by ionic liquids, Chem. Data Collect., 33 (2021) 100717, doi: 10.1016/j.cdc.2021.100717.
[28] T. Ngoya, E.F. Aransiola, O. Oyekola, Optimisation of biodiesel production from waste vegetable oil and eggshell ash, S. Afr. J. Chem. Eng., 23 (2017) 145–156.
[29] F. Kargi, S. Ozmihci, Biosorption performance of powdered activated sludge for removal of different dyestuffs, Enzyme Microb. Technol., 35 (2004) 267–271.
[30] A.I. Adeogun, E.A. Ofudje, M.A. Idowu, S.A. Ahmed, Kinetic, thermodynamic and isotherm parameters of biosorption of Cr(VI) and Pb(II) ions from aqueous solution by biosorbent prepared from corncob biomass, Indian J. Inorg. Chem., 7 (2012) 119–129.
[31] I. Langmuir, The constitution and fundamental properties of solids and liquids, J. Am. Chem. Soc., 38 (1916) 2221–2295.
[32] M.J. Temkin, V. Pyzhev, Recent modifications to Langmuir isotherms, Acta Physiochim. USSR, 12 (1940) 217–222.
[33] E.A. Ofudje, O.D. Williams, K.K. Asogwa, A.O. Awotula, Assessment of Langmuir, Freundlich and Dubinin–Radushhkevich adsorption isotherms in the study of the biosorption of Mn(II) ions from aqueous solution by untreated and acid-treated corn shaft, Int. J. Sci. Eng. Res., 4 (2013) 1628–1634.
[34] O. Redlich, D.L. Peterson, A useful adsorption isotherm, J. Phys. Chem., 63 (1959) 1024, doi: 10.1021/j150576a611.
[35] R. Sips, Combined form of Langmuir and Freundlich equations, J. Chem. Phys., 16 (1948) 490–495.
[36] B. Meriem, A. Fatima, Comparative adsorption isotherms and modeling of methylene blue onto activated carbons, Appl. Water Sci., 1 (2011) 111–117.
[37] S. Lagergren, About the theory of so-called adsorption of soluble substances, K. Sven. Vetenskapsakad. Handl., 24 (1898) 1–39.
[38] Y.S. Ho, Citation review of Lagergen kinetic rate equation on adsorption reactions, Scientometrics, 59 (2004) 171–177.
[39] M.J.D. Low, Kinetics of chemisorption of gases on solids, Chem. Rev., 60 (1960) 267–312.
[40] W.J. Weber, J.C. Morris, Kinetics of adsorption on carbon from solution, J. Sanit. Eng. Div., Am. Soc. Chem. Eng., 89 (1963) 31–59.
[41] U. Anjaneyulu, S. Sasikumar, Bioactive nanocrystalline wollastonite synthesized by sol–gel combustion method by using eggshell waste as calcium source, Bull. Mater. Sci., 37 (2014) 207–212.
[42] A.I. Adeogun, A.E. Ofudje, M.A. Idowu, S.O. Kareem, Facile development of nano size calcium hydroxyapatite based ceramic from eggshells: synthesis and characterization, Waste Biomass Valorization, 4 (2017) 1–5, doi: 10.1007/s12649-017-9891-3.
[43] P. Himanshu, R.T. Vashi, A study on the removal of Toluidine blue dye from aqueous solution by adsorption onto neem leaf powder, Int. Sch. Sci. Res. Innovation, 4 (2010) 674–679.
[44] K.A. Sibel, O. Ozge, A. Senol, A. Husamettin, The adsorption kinetics and removal of cationic dye, Toluidine blue O, from aqueous solution with Turkish zeolite, J. Hazard. Mater., 151 (2008) 213–220.
[45] M.A. Rauf, M.Q. Shahnaz, A. Sarmadia, K.M. Al-Mansoori, Adsorption studies of Toluidine blue from aqueous solutions onto gypsum, Chem. Eng. J., 150 (2009) 90–95.
[46] G. Lei, L. Guiying, L. Junshen, M. Songmei, Z. Jinfeng, Kinetic and equilibrium studies on adsorptive removal of Toluidine blue by water-insoluble starch sulfate, J. Chem. Eng. Data, 56 (2011) 1875–1881.

[47] R. Ahmad, Studies on adsorption of crystal violet dye from aqueous solution onto coniferous pinus bark powder (CPBP), J. Hazard. Mater., 171 (2009) 767–773.
[48] N. Barka, S. Qourzal, A. Assabbane, A. Nounah, Y. Aitichou, Adsorption of disperse blue SBL dye by synthesized poorly crystalline hydroxyapatite, J. Environ. Sci., 20 (2008) 1268–1272.
[49] M. Khalid, M.I. Azharul, M. Anastasios, A. Triantafillos, V. Tiverios, Adsorption of direct yellow 27 from water by poorly crystalline hydroxyapatite prepared via precipitation method, Desal. Water Treat., 41 (2012) 170–178.
[50] E.A. Ofudje, B. Akinbile, A.O. Awotula, G.O. Oladipo, E.A. Adedapo, Kinetic studies of thiocyanate ions removal from aqueous solution using carbonaceous guinea-corn, J. Sci. Res., 14 (2015) 94–101.
[51] E.A. Ofudje, A.O. Awotula, G.V. Hambate, F. Akinwunmi, S.O. Alayande, O.D. Olukanni, Acid activation of groundnut husk for copper adsorption: kinetics and equilibrium studies, Desal. Water Treat., 86 (2017) 240–251.
[52] K. Kannan, M.M. Sundaram, Kinetics and mechanism of removal of methylene blue by adsorption on various carbons—comparative study, Dyes Pigm., 51 (2015) 25–40.
[53] C. Duran, D. Ozdes, A. Gundogdu, H.B. Senturk, Kinetics and isotherm analysis of basic dyes adsorption onto almond shell (*Prunus dulcis*) as a low cost adsorbent, J. Chem. Eng. Data, 56 (2011) 2136–2147.
[54] M.S. Chiou, H.Y. Li, Adsorption behavior of reactive dye in aqueous solution on chemical cross-linked chitosan beads, Chemosphere, 50 (2003) 1095–1105.
[55] M.-H. Baek, C.O. Ijagbemi, S.-J. O, D.-S. Kim, Removal of Malachite Green from aqueous solution using degreased coffee bean, J. Hazard. Mater., 176 (2010) 820–828.
[56] S. Soni, P. Kumar Bajpai, D. Bharti, J. Mittal, C. Arora, Removal of crystal violet from aqueous solution using iron based metal organic framework, Desal. Water Treat., 205 (2020) 386–399.
[57] X. Li, J.L. Zheng, L. Huang, O. Zheng, Z. Lin, L. Guo, B. Qiu, G. Chen, Adsorption removal of crystal violet from aqueous solution using a metal-organic frameworks material, copper coordination polymer with dithiooxamide, J. Appl. Polym. Sci., 129 (2013) 2857–2864.
[58] S. Loera-Serna, J. Garcia-Ortiz, E. Ortiz, Dyes adsorption on $Cu_3(BTC)_2$ metal-organic framework, Adv. Mater.: TechConnect Briefs, 1 (2016) 331–334.
[59] R. Malik, D.S. Ramteke, S.R. Wate, Adsorption of malachite green on groundnut shell waste based powdered activated carbon, Waste Manage., 27 (2007)1129–1138.
[60] V.K. Gupta, S.K. Srivastava, D. Mohan, Equilibrium uptake, sorption dynamics, process optimization, and column operations for the removal and recovery of malachite green from wastewater using activated carbon and activated slag, Ind. Eng. Chem. Res., 36 (1997) 2207–2218.